

CT differentiation of enlarged mediastinal lymph node due to anthracosis from metastatic lymphadenopathy: a comparative study proven by endobronchial US-guided transbronchial needle aspiration

Johannes Kirchner, Michael Broll, Phillip Müller, Natalia Pomjanski, Stepfan Biesterfeld, Dieter Liermann, Ralph Kickuth

PURPOSE

Anthracosis often results in mediastinal nodal enlargement. The aim of this comparative study was to evaluate if it is possible to differentiate endobronchial ultrasound-guided transbronchial needle aspiration (EBUS-TBNA) proven anthracotic lymph nodes from malignant lymph node enlargement by means of multislice computed tomography (MSCT).

METHODS

We compared the MSCT findings of 89 enlarged lymph nodes due to anthracosis with 54 malignant lymph nodes (non-small cell lung cancer 75.9%, small cell lung cancer 18.5%, and non-Hodgkin lymphoma 5.6%). The lymph nodes were assessed for density (calcification, fat, and necrosis), shape (oval, round), contrast enhancement, and contour (sharp, ill-defined).

RESULTS

Malignant lymph nodes showed significantly greater axis diameters ($P < 0.001$). Both anthracotic and malignant nodes were most often oval (86.5% of all malignant nodes vs. 81.5% of all anthracotic nodes, $P = 0.420$) and showed confluence in a remarkable percentage (28.1% vs. 42.6%, $P = 0.075$). Anthracotic nodes showed calcifications more often (18% vs. 0%, $P < 0.001$). Malignant lymph nodes showed a significantly greater short and long axis diameter ($P < 0.001$), and they had a higher frequency of ill-defined contours (27.8% vs. 2.2%, $P < 0.001$) and contrast enhancement (27.8% vs. 5.6%, $P < 0.001$). Nodal necrosis, which appeared in one third of the malignant nodes, was not observed in anthracosis (35.2% vs. 0%, $P < 0.001$). Confluence of enlarged lymph nodes was seen in malignant lymph nodes (42.6%), as well as in lymph node enlargement due to anthracosis (28.1%, $P = 0.075$).

CONCLUSION

Our results show that there are significant differences in MSCT findings of malignant enlarged lymph nodes and benign lymph node enlargement due to anthracosis.

Anthracosis is characterized by alterations not only of the lung parenchyma and bronchioles but also of the lymphatic system, resulting in chronic lymphadenopathy and nodal enlargement (1). Since finding of enlarged mediastinal lymph nodes on computed tomography (CT) may raise the suspicion of metastasis in patients with a known primary neoplasm (2, 3), and lymph node anthracosis may appear as false positive on positron emission tomography (PET) (4–6), it can confuse clinicians in staging of lung cancer patients.

The aim of this comparative study of endobronchial ultrasound-guided transbronchial needle aspiration (EBUS-TBNA) and chest CT was to evaluate whether it is possible to differentiate enlarged anthracotic lymph nodes from malignant lymph node enlargement by means of CT. To the best of our knowledge, this study seems to be the first to deal with the differential diagnosis of enlarged anthracotic and malignant lymph nodes in this setting.

Methods

Patients

This comparative study on lymph node enlargement due to anthracosis and metastatic disease was designed as a follow-up examination to our recently published study on CT findings in mediastinal lymph node anthracosis (1). For this purpose we performed an analysis on 49 consecutive patients with EBUS-TBNA confirmed diagnosis of lymph node anthracosis and 30 consecutive patients with malignant lymph node enlargement without any finding of anthracotic pigment. The main inclusion criterion for patients with anthracosis was a deposition of anthracotic material in the cytological specimen; an additional bronchoscopic finding indicating anthracofibrosis as bronchial narrowing or anthracotic tattoos was not mandatory. The study was approved by the ethics committee of our university and was compliant to the Health Insurance Portability and Accountability Act of 1996.

Computed tomography

Contrast-enhanced multislice CT examinations were carried out using two state-of-the-art CT systems (Siemens Somatom 64, Siemens Medical Solutions, and Toshiba Aquilion 64, Toshiba Medical Systems). Images were obtained at full inspiration predominantly during the venous phase using a 64×0.75 mm slice collimation with a tube voltage of 120 kV. The tube current (mA) was adjusted in relation to patient attenuation by means of the Care Dose® modus (Siemens Medical Solutions) or the Sure Exposure® modus (Toshiba Medical Systems). The reconstruction slice thickness was 3–5 mm; in general reconstruction

From the Department of Diagnostic and Interventional Radiology (J.K. ✉ Kirchner@akh-hagen.de, PM.), Allgemeines Krankenhaus Hagen, Germany; the Department of Medicine (M.B.), Klinikum Wedau Duisburg, Germany; the Department of Cytopathology (N.P., S.B.), Heinrich Heine Universität Düsseldorf, Germany; the Department of Diagnostic and Interventional Radiology and Nuclearmedicine (D.L.), Katholisches Marienhospital Herne Universitätsklinikum der Ruhr-Universität Bochum, Germany; the Department of Radiology (R.K.), Universitätsklinikum Würzburg, Germany.

Received 20 March 2014, revision requested 21 April 2014, final revision received 18 August 2014, accepted 28 August 2014.

Published online 23 January 2015.
DOI 10.5152/dir.2014.14112

planes comprised the axial, coronal, and sagittal views.

Biopsy

EBUS-TBNA was performed using a linear array 7.5 MHz ultrasonic bronchoscope (CP EBUS, Olympus Medical Systems) with a 90° angle of view. TBNA was performed under real-time ultrasound-guidance using a 22G needle (model NA 201 SX 402, Olympus Medical Systems).

Image evaluation

The retrospective evaluation was performed consensually by two board certified radiologists (J.K. and R.K.). Lymph node enlargement was defined as showing a size of more than 7–11 mm on the short axis based on the American Thoracic Society (ATS) definitions (7). Enlarged mediastinal lymph nodes were assessed for density (calcification, fat, necrosis), shape (oval, round) and contour (sharp, ill-defined). Nodal necrosis was considered present when an enlarged lymph node showed ill-defined low-attenuation areas. Noticeable lymph node enhancement was determined as nodal density >60 HU in CT. The evaluation comprised a correlation of CT findings and EBUS-reports to determine which lymph nodes in CT had been aspirated by TBNA.

Statistical analysis

Descriptive data were presented as means with ranges, if appropriate; categorical data were given as counts and percentages. We performed t tests, chi-square tests, and Fischer's exact test by means of a specialized computer algorithm (MedCalc® Software) to correlate different CT findings such as lymph node size, shape, contour, etc., with the histological findings in EBUS-TBNA. Significance was set at a *P* value of less than 0.05.

Results

Of 79 retrospectively enrolled patients, cytologically-confirmed anthracosis (Fig. 1) was diagnosed in 89 lymph nodes in 49 patients. In all patients EBUS-TBNA was performed because of the *a priori* diagnosis of mediastinal lymph node malignancy on previous chest CT.

Table 1. Sample characteristics

	Anthracosis	Malignant
Patients, n	49	30
Examined lymph nodes, n	89	54
Age (years), mean	65.7	65.9
Gender (male:female)	0.69:0.31	0.6:0.4

Age and gender distribution was not significantly different between the study groups (*P* = 0.940 and *P* = 0.546, respectively).

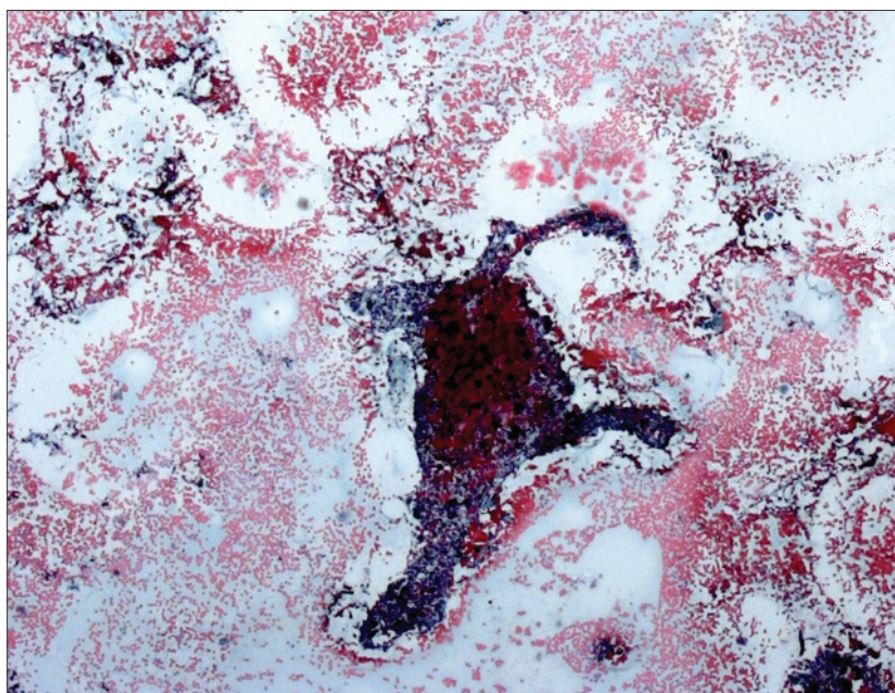


Figure 1. EBUS-TBNA in an enlarged anthracotic lymph node. Cytologic specimen shows a fibrous fragment of a lymph node with deposition of anthracotic pigment in macrophages and in the extracellular space. Papanicolaou staining, 12x10.

Anthracosis patients had a mean age of 65.7 years (range, 29–88 years) with a 0.69:0.31 predominance of the male gender (Table 1). The control group (n=30) had a comparable age distribution (mean age, 65.9 years; range, 19–96 years) and gender ratio (0.6:0.4). The groups were not significantly different in terms of age (*P* = 0.940) or gender (*P* = 0.546).

Retrospective analysis of the electronic health records of 49 patients with lymph node enlargement due to anthracosis revealed that seven patients had accompanying malignancy (five cases of bronchial cancer, two cases of non-Hodgkin lymphoma). In 26 patients severe nicotine abuse was documented and only two patients had occupational exposure to dust.

In the control group, EBUS-TBNA revealed malignancy in 54 lymph nodes: 18 non-small cell lung cancer not otherwise specified (33.3%), 10 small cell lung cancer (18.5%), nine squamous cell carcinoma (16.7%), nine adenocarcinoma (16.7%), five large cell lung cancer (9.3%), and three non-Hodgkin lymphoma (5.6%).

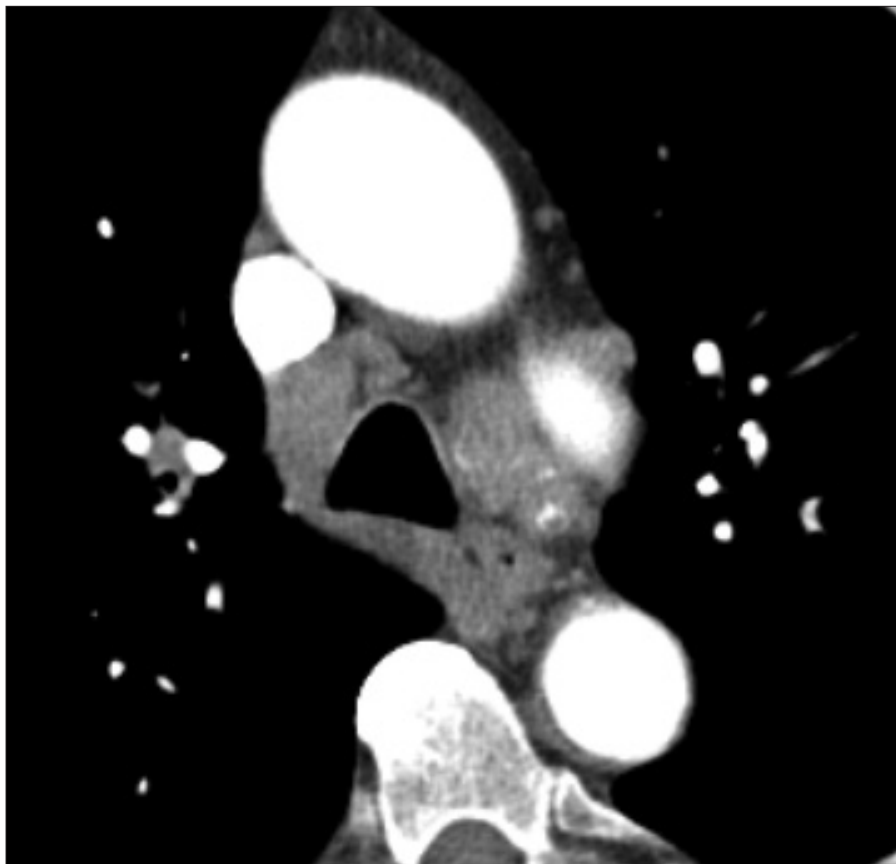
As presented in Table 2, the most common site of lymph node aspiration was ATS region 7 (54/143 nodes, 37.9%). Additionally, EBUS-TBNA was more often performed on the nodal regions on the right side (68 vs. 21 nodes). This held true for anthracotic lymph nodes as well as malignant nodes.

The short axis of the histologically-proven anthracotic lymph nodes

Table 2. Distribution of EBUS-confirmed lymph nodes on ATS regions

ATS regions	Anthracosis n (%)	Malignant n (%)	Total n (%)
2R	3 (3.4)	1 (1.9)	4 (2.8)
2L	1 (1.1)	0 (0)	1 (0.7)
4R	8 (9.0)	5 (9.3)	13 (9.1)
4L	5 (5.6)	2 (3.7)	7 (4.9)
7	35 (39.3)	19 (35.2)	54 (37.8)
10R	19 (21.3)	12 (22.2)	31 (57.4)
10L	2 (2.2)	5 (9.3)	7 (4.9)
11R	13 (14.6)	7 (12.9)	20 (14.0)
11L	3 (3.4)	3 (5.6)	6 (4.2)
Total	89 (100)	54 (100)	143 (100)

EBUS, endobronchial ultrasound; ATS, American Thoracic Society.

**Figure 2.** CT image reveals confluence of enlarged lymph nodes in ATS regions 4R/10R and 4L/10L, some of them showing subtle calcifications.

had a mean diameter of 11.1 ± 3.98 mm (6–23 mm), while the long axis had a mean diameter of 16.5 ± 6.09 mm (8–31 mm). Malignant lymph nodes showed a mean short axis diameter of 15.3 ± 6.43 mm (5–36 mm) and a mean long axis diameter of 21.6 ± 9.07 mm (4–45 mm).

The differences regarding short and long axis diameters were found to be statistically significant ($t=4.938$ and $t=4.046$, respectively; $P < 0.001$).

Most lymph nodes with signs of anthracosis showed an oval shape (77/89 nodes, 86.5%); seven nodes had

a round shape (7.9%) and five nodes had a polycyclic shape (5.6%). In the control group, a similar frequency of different shapes was found: 44 oval (81.5%), eight round-shaped (14.8%), and two polycyclic (3.7%). Shape distribution was not significantly different between the groups ($P = 0.438$).

Confluence of two or more enlarged lymph nodes was seen in 25 nodes with anthracosis and in 23 malignant nodes (28.1% vs. 42.6%, $P = 0.075$) (Fig. 2). Contrast enhancement was documented in five of the anthracotic lymph nodes and 15 of the malignant lymph nodes; this difference was significant (5.6% vs. 27.8%, $P < 0.001$). A central hypodensity due to fatty involution was seen in two of the anthracotic lymph nodes and in none of the malignant nodes (2.2% vs. 0%, $P = 0.52$). Lymph node necrosis was not present in lymph node anthracosis, but it was present in 19 of 54 malignant nodes, which indicated a significant difference (0% vs. 35.2%, $P < 0.001$) and a high positive predictive value (PPV=100%) for predicting malignancy (Fig. 3, Table 3).

CT revealed calcification-like hyperdensities in 16 of 89 anthracotic nodes (18.0%, Fig. 4); this finding was not seen in any of the malignant lymph nodes ($P < 0.001$). Ill-defined lymph nodes were seen significantly more often in malignant nodes (15/54, 27.8%) than in anthracosis (2/89, 2.2%) ($P < 0.001$; PPV, 88.2%).

Discussion

There have been many studies to differentiate benign mediastinal lymph nodes from malignant ones. Most often a coherent appearance of malignancy and enlarged lymph nodes was demonstrated on CT (8, 9). Usually a short axis diameter > 1 cm is considered as the standard threshold for a suspicious lymph node, but metastases have been found in up to 20% of small nodes in patients with clinical stage cT1N0 and cT2N0, and only about 50% of the nodes with a diameter of 1.5 cm to 2 cm are metastatic (3). This results in low sensitivities (50%–65%) and specificities (65%–85%) of CT in the assessment of mediastinal lymph-node involvement (3). Moreover, it was shown that

Table 3. CT findings in enlarged lymph nodes due to anthracosis or malignant conditions (control group)

		Anthracosis n=89	Malignant n=54	P	PPV (%)	NPV (%)
Size (mm), mean±SD	Short axis	11.1±3.98	15.3±6.43	<0.001	-	-
	Long axis	16.5±6.09	21.6±9.07	<0.001	-	-
Shape	Oval	77 (86.5)	44 (81.5)	0.438	36.4	54.5
	Round	7 (7.9)	8 (14.8)		53.3	64.1
	Polycyclic	5 (5.6)	2 (3.7)		28.6	61.8
Margin	Ill-defined	2 (2.2)	15 (27.8)	<0.001	88.2	69.0
	Confluence	25 (28.1)	23 (42.6)	0.075	47.9	67.3
Contrast enhancement		5 (5.6)	15 (27.8)	<0.001	75.0	68.3
Calcification		16 (18)	0	<0.001	0.06	57.9
Fat		2 (2.2)	0	0.527	0	61.7
Necrosis		0 (0)	19 (35.2)	<0.001	100.0	71.8

Unless otherwise noted, data are presented as n (%).

PPV, positive predictive value; NPV, negative predictive value.

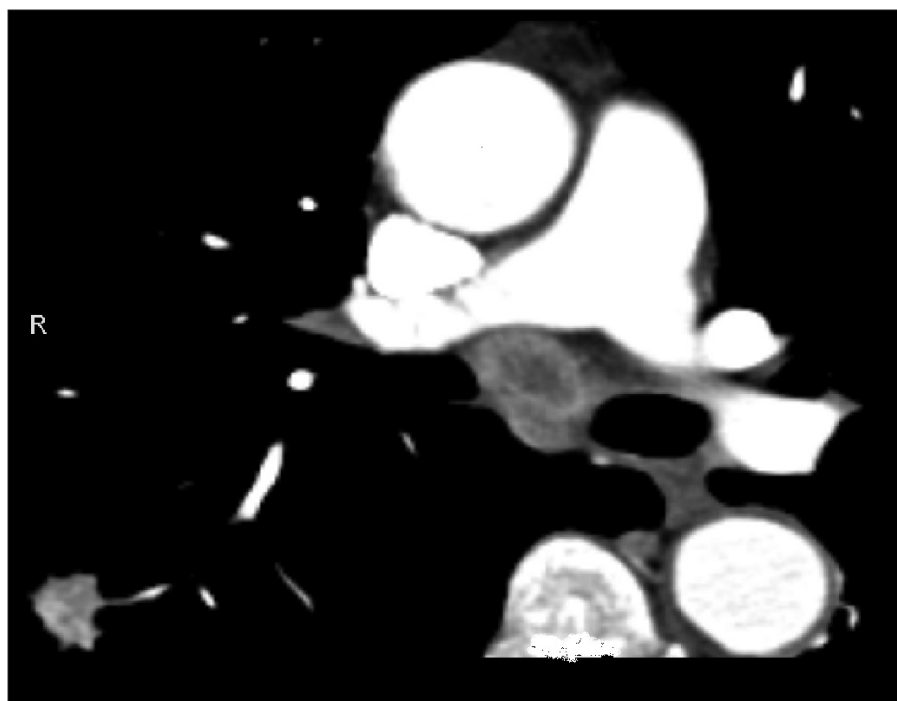


Figure 3. CT image reveals an enlarged lymph node in ATS Region 7 showing central colliquation. Pulmonary mass is seen in the right lower lobe (EBUS-TBNA confirmed small-cell lung carcinoma).

thoracic lymph node enlargement can also be found in multiple benign conditions such as granulomatous disease (10), pneumoconiosis (11), or even heart failure (12). In a recently published comparative study on 44 heavy smokers and 44 nonsmokers we demonstrated that enlarged mediastinal lymph nodes may occur in up to 52% of heavy smokers, especially in those with severe bronchitis (13). In that study we assumed that lymph

node enlargement in smokers may be caused by a deposition of anthracotic material and dust-induced response. Anthracosis is a form of pneumoconiosis which is not only caused by coal dust, but also by other environmental factors such as air pollution, biomass fuels used extensively for cooking (“hut lung”), and cigarette smoking (13–18). It has been recently demonstrated that the presence of microscopic anthracotic pigment in EBUS-TBNA

of enlarged lymph nodes is negatively associated with lymph node malignancy (19). The findings of the present study confirm the hypothesis that anthracosis may result in considerable enlargement of mediastinal lymph nodes up to 23 mm in short axis diameter. Nevertheless, the mean diameter of malignant enlarged lymph nodes is significantly larger than anthracotic lymph nodes. In addition, ill-defined margins are found significantly more often in malignant lymph nodes. This finding is in contrast to the report of Sakai et al. (20) indicating that the ill-defined margin of an enlarged lymph node is a relatively common feature in inflammatory changed lymph nodes (20). While some authors suggested nodal confluence as a reliable indicator of malignancy (21), surprisingly in our study this finding was observed in nearly one third of the anthracotic enlarged lymph nodes and no significant difference was found between the two groups in terms of nodal confluence.

Lymph node calcification was observed significantly more often in anthracotic nodes than in malignant lymph node enlargement. The finding that lymph node calcifications were observed in one fourth of the anthracotic lymph nodes is in accordance with the literature (1, 14, 22). Therefore this finding might be judged as a reliable indicator for benign lymph node enlargement.

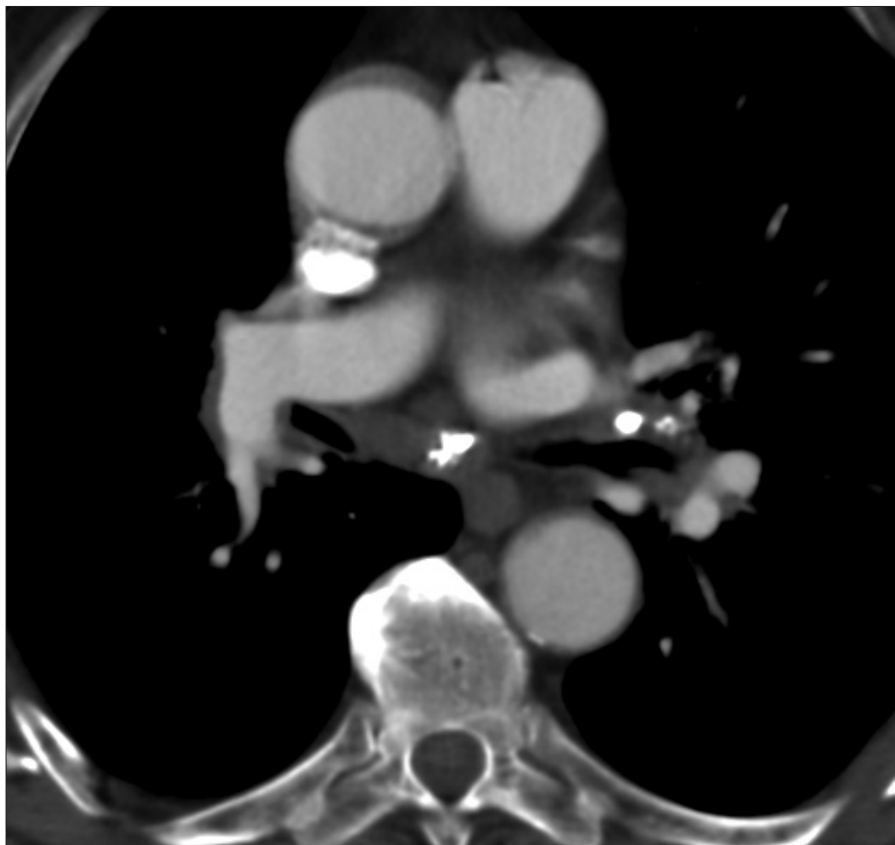


Figure 4. CT image demonstrating extensive calcifications in enlarged lymph nodes with EBUS-TBNA confirmed anthracosis.

On the other hand lymph node necrosis, which has been reported to be present both in malignancy (23, 24) and in nodal inflammation (25, 26), was seen in one third of the malignant lymph nodes compared with none of the anthracotic nodes. This would result in a PPV of 100%; and consequently, nodal necrosis might be interpreted as a strong indicator for nodal malignancy. Nevertheless, this finding must be limited to the specific setting of our study. We report on a population with a very low incidence of tuberculosis. Tuberculosis is a well-known cause of necrotic mediastinal lymph nodes (27) and an association between anthrocofibrosis and tuberculosis has been described in the literature (28). Therefore the finding of nodal necrosis as a strong indicator for nodal malignancy cannot be generalized, at least for countries with a high incidence of tuberculosis.

In accordance with Volterrani et al. (29), malignant lymph nodes showed contrast enhancement significantly more often in our study; however,

other authors found contrast enhancement to be typical for nodal inflammation as well (26). There were some limitations to our study. First, the sample size was small, preventing generalization of our results. Second, the study design was retrospective, and therefore, some clinical data may be questioned (e.g., percentage of smokers). Another problem resulting from this retrospective setting is the use of different reconstruction slice thicknesses, which might have influenced the diameter measurements. Also, not all enlarged nodes present on CT could have been evaluated. Therefore we consider our results preliminary.

In conclusion, the results of the present study show that there are some differences in CT findings of malignant enlarged lymph nodes and lymph node enlargement due to anthracosis. While anthracotic nodes show calcifications more often, malignant lymph nodes are significantly more often ill-defined and show contrast enhancement significantly more often. Nodal necrosis which appears in one third of

the malignant nodes was not observed in anthracosis and seems to be a strong indicator for malignancy.

Conflict of interest disclosure

The authors declared no conflicts of interest.

References

1. Kirchner J, Mueller P, Broll M, et al. Chest CT findings in EBUS-TBNA-proven anthracosis in enlarged mediastinal lymph nodes. *Rofo* 2014; 186:1122–1126. [\[CrossRef\]](#)
2. Parmaksız ET, Caglayan B, Salepci B, et al. The utility of endobronchial ultrasound-guided transbronchial needle aspiration in mediastinal or hilar lymph node evaluation in extrathoracic malignancy: Benign or malignant? *Ann Thorac Med* 2012; 7:210–214. [\[CrossRef\]](#)
3. Toloza EM, Harpole L, Detterbeck F, McCrory DC. Invasive staging of non-small cell lung cancer: a review of the current evidence. *Chest* 2003; 123:157S–166S. [\[CrossRef\]](#)
4. Cheng NM, Yeh TW, Ho KC, et al. False positive F-18 FDG PET/CT in neck and mediastinum lymph nodes due to anthracosis in a buccal cancer patient. *Clin Nucl Med* 2011; 36:963–964. [\[CrossRef\]](#)
5. Saydam O, Gokce M, Kilicgun A, Tanriverdi O. Accuracy of positron emission tomography in mediastinal node assessment in coal workers with lung cancer. *Med Oncol* 2012; 29:589–594. [\[CrossRef\]](#)
6. Reichert M, Bensadoun ES. PET imaging in patients with coal workers pneumoconiosis and suspected malignancy. *J Thorac Oncol* 2009; 4:649–651. [\[CrossRef\]](#)
7. Glazer GM, Gross BH, Quint LE, Francis IR, Bookstein FL, Orringer MB. Normal mediastinal lymph nodes: number and size according to American Thoracic Society mapping. *AJR Am J Roentgenol* 1985; 144:261–265. [\[CrossRef\]](#)
8. de Langen AJ, Raijmakers P, Riphagen I, Paul MA, Hoekstra OS. The size of mediastinal lymph nodes and its relation with metastatic involvement: a meta-analysis. *Eur J Cardiothorac Surg* 2006; 29:26–29. [\[CrossRef\]](#)
9. Quint LE, Francis IR. Radiologic staging of lung cancer. *J Thorac Imaging* 1999; 14:235–246. [\[CrossRef\]](#)
10. Hunt BM, Vallières E, Buduhan G, Aye R, Louie B. Sarcoidosis as a benign cause of lymphadenopathy in cancer patients. *Am J Surg* 2009; 197:629–632. [\[CrossRef\]](#)
11. Baldwin DR, Lambert L, Pantin CF, Prowse K, Cole RB. Silicosis presenting as bilateral hilar lymphadenopathy. *Thorax* 1996; 51:1165–1167. [\[CrossRef\]](#)
12. Ardekani MS, Issa M, Green L. Diagnostic and economic impact of heart failure induced mediastinal lymphadenopathy. *Int J Cardiol* 2006; 109:137–138. [\[CrossRef\]](#)
13. Kirchner J, Kirchner EM, Goltz JP, Obermann A, Kickuth R. Enlarged hilar and mediastinal lymph nodes in chronic obstructive pulmonary disease. *J Med Imaging Radiat Oncol* 2010; 54:333–338. [\[CrossRef\]](#)
14. Bilici A, Erdem T, Boysan SN, et al. A case of anthracosis presenting with mediastinal lymph nodes mimicking tuberculous lymphadenitis or malignancy. *Eur J Intern Med* 2003; 14:444–446. [\[CrossRef\]](#)

15. Gold JA, Jagirdar J, Hay JG, Addrizzo-Harris DJ, Naidich DP, Rom WN. Hut lung. A domestically acquired particulate lung disease. *Medicine (Baltimore)* 2000; 79:310–317. [\[CrossRef\]](#)
16. Kim YJ, Jung CY, Shin HW, Lee BK. Biomass smoke induced bronchial anthracofibrosis: presenting features and clinical course. *Respir Med* 2009; 103:757–765. [\[CrossRef\]](#)
17. Klaaver M, Kars AH, Maat AP, den Bakker MA. Pseudomediastinal fibrosis caused by massive lymphadenopathy in domestically acquired particulate lung disease. *Ann Diagn Pathol* 2008; 12:118–121. [\[CrossRef\]](#)
18. Naccache JM, Monnet I, Nunes H, et al. Anthracofibrosis attributed to mixed mineral dust exposure: report of three cases. *Thorax* 2008; 63:655–657. [\[CrossRef\]](#)
19. Park YS, Lee J, Pang JC, et al. Clinical implication of microscopic anthracotic pigment in mediastinal staging of non-small cell lung cancer by endobronchial ultrasound-guided transbronchial needle aspiration. *J Korean Med Sci* 2013; 28:550–554. [\[CrossRef\]](#)
20. Sakai O, Curtin HD, Romo LV, Som PM. Lymph node pathology. Benign proliferative, lymphoma, and metastatic disease. *Radiol Clin North Am* 2000; 38:979–998. [\[CrossRef\]](#)
21. Stern WB, Silver CE, Zeifer BA, Persky MS, Heller KS. Computed tomography of the clinically negative neck. *Head Neck* 1990; 12:109–113. [\[CrossRef\]](#)
22. Gross BH, Schneider HJ, Proto AV. Eggshell calcification of lymph nodes: an update. *AJR Am J Roentgenol* 1980; 135:1265–1268. [\[CrossRef\]](#)
23. Saindane AM. Pitfalls in the staging of cervical lymph node metastasis. *Neuroimaging Clin N Am* 2013; 23:147–166. [\[CrossRef\]](#)
24. Zoumalan RA, Kleinberger AJ, Morris LG, et al. Lymph node central necrosis on computed tomography as predictor of extracapsular spread in metastatic head and neck cell carcinoma: pilot study. *J Laryngol Otol* 2010; 124:1284–1288. [\[CrossRef\]](#)
25. Je BK, Kim MJ, Kim SB, Park DW, Kim TK, Lee NJ. Detailed nodal features of cervical tuberculous lymphadenitis on serial neck computed tomography before and after chemotherapy: focus on the relation between clinical outcomes and computed tomography features. *J Comput Assist Tomogr* 2005; 29:889–894. [\[CrossRef\]](#)
26. Lee Y, Park KS, Chung SY. Cervical tuberculous lymphadenitis: CT findings. *J Comput Assist Tomogr* 1994; 18:370–375. [\[CrossRef\]](#)
27. Özgül MA, Cetinkaya E, Tutar N, Özgül G, Onaran H, Bilaceroglu S. Endobronchial ultrasound-guided transbronchial needle aspiration for the diagnosis of intrathoracic lymphadenopathy in patients with extrathoracic malignancy: A study in a tuberculosis-endemic country. *J Cancer Res Ther* 2013; 9:416–421. [\[CrossRef\]](#)
28. Bekci TT, Maden E, Emre L. Bronchial anthracofibrosis case with endobronchial tuberculosis. *Int J Med Sci* 2011; 8:84–87. [\[CrossRef\]](#)
29. Volterrani L, Mazzei MA, Banchi B, et al. MSCT multi-criteria: a novel approach in assessment of mediastinal lymph node metastases in non-small cell lung cancer. *Eur J Radiol* 2011; 79:459–466. [\[CrossRef\]](#)